Appl Microbiol Biotechnol
DOI 10.1007/s00253-016-7865-1

ENVIRONMENTAL BIOTECHNOLOGY

Taxonomical and functional microbial community dynamics in an Anammox-ASBR system under different Fe (III) supplementation

Xiao Wang[1] · **Duntao Shu**[2] · **Hong Yue**[3]

Received: 8 August 2016 / Revised: 30 August 2016 / Accepted: 13 September 2016

Abstract In the present study, we explored the metabolic versatility of anaerobic ammonium oxidation (anammox) bacteria in a variety of Fe (III) concentrations. Specifically, we investigated the impacts of Fe (III) on anammox growth rates, on nitrogen removal performance, and on microbial community dynamics. The results from our short-term experiments revealed that Fe (III) concentrations (0.04–0.10 mM) significantly promote the specific anammox growth rate from 0.1343 to 0.1709 d^{-1}. In the long-term experiments, the Anammox-anaerobic sequencing batch reactor (ASBR) was operated over 120 days and achieved maximum NH_4^+-N, NO_2^--N, and TN efficiencies of 90.98 ± 0.35, 93.78 ± 0.29, and 83.66 ± 0.46 %, respectively. Pearson's correlation coefficients between anammox-(*narG* + *napA*), anammox-*nrfA*, and anammox-FeRB all exceeded $r = 0.820$ ($p < 0.05$), confirming an interaction and ecological association among the nitrogen and iron-cycling-related microbial communities. Illumina MiSeq sequencing indicated that *Chloroflexi* (34.39–39.31 %) was the most abundant phylum in an Anammox-ASBR system, followed by *Planctomycetes* (30.73–35.31 %), *Proteobacteria* (15.40–18.61 %), and *Chlorobi* (4.78–6.58 %). Furthermore, we found that higher Fe (III) supplementation (>0.06 mM) could result in the community succession of anammox species, in which *Candidatus* Brocadia and *Candidatus* Kuenenia were the dominant anammox bacteria species. Combined analyses indicated that the coupling of anammox, dissimilatory nitrogen reduction to ammonium, and iron reduction accounted for nitrogen loss in the Anammox-ASBR system. Overall, the knowledge gained in this study provides novel insights into the microbial community dynamics and metabolic potential of anammox bacteria under Fe (III) supplementation.

Keywords Anammox · Fe (III) · MiSeq sequencing · Microbial community · Biological nitrogen removal

Xiao Wang and Hong Yue contributed equally to this work.

Electronic supplementary material The online version of this article (doi:10.1007/s00253-016-7865-1) contains supplementary material, which is available to authorized users.

✉ Duntao Shu
D.T.Shu_xjtu@outlook.com

[1] School of Chemical Engineering, Qinghai University, Xining, Qinghai 810016, China

[2] State Key Laboratory of Crop Stress Biology in Arid Areas, College of Life Sciences, Northwest A&F University, Yangling, Shaanxi 712100, China

[3] State Key Laboratory of Crop Stress Biology in Arid Areas, College of Agronomy and Yangling Branch of China Wheat Improvement Center, Northwest A&F University, Yangling, Shaanxi 712100, China

Introduction

Anaerobic ammonium oxidizing (anammox) bacteria, which were discovered in a denitrifying fluidized bed reactor in the early 1990s, have the unique ability to couple ammonium and nitrite to form N_2 (Strous et al. 1999; van de Graaf et al. 1997). As chemolithoautotrophic bacteria, anammox bacteria are affiliated with a monophyletic group in the phylum *Planctomycetes* (Strous et al. 1999), and five candidate genera within it including *Candidatus* Brocadia, *Candidatus* Kuenenia, *Candidatus* Scalindua, *Candidatus* Anammoxoglobus, and *Candidatus* Jettenia have been detected by using 16S and 23S ribosomal ribonucleic acid (rRNA) gene sequencing (Kartal et al. 2013; Kuenen 2008). Anammox-related techniques have been successfully used to

Published online: 01 October 2016

remove nitrogen applied in nearly 100 full-scale wastewater treatment plants due to their high efficiencies and low cost (Guo et al. 2016; Lotti et al. 2015; Van der Star et al. 2007). However, the very low growth rate of anammox bacteria and their sensitivity to environmental factors, such as heavy metals, organic matter, pH, and DO (dissolved oxygen) (Jin et al. 2012), have been considered major obstacles for the mainstream and side-stream applications of the anammox-related process.

Many strategies, including wash-out methods, PVA-SA gel immobilization, Fe (II) addition, and an ultrasound field (Ali et al. 2015; Duan et al. 2011; Gao et al. 2014; Liu and Horn 2012; Liu and Ni 2015; Qiao et al. 2013), have therefore been developed to enhance the growth rate and cellular yield of anammox bacteria. Moreover, several incubation systems for anammox bacteria have been developed, such as sequencing batch reactor (SBR), upflow anaerobic sludge blanket (UASB), gas-lift reactors, fluidized bed, membrane bioreactor (MBR) (Table S1), and rotating biological contactors (Kartal et al. 2012; Schmidt et al. 2004; Van de Graaf et al. 1996). Strengthening anammox activity with low-energy input and high feasibility is a highly sought after research goal in the present and for the future.

As the fourth most abundant element of the Earth's crust, iron (Fe) is of great application value (Melton et al. 2014) and iron is often encountered in wastewaters such as landfill leachates, power plants, and metal industrial wastewaters. In addition, ferric salts are often utilized as precipitants in the process of wastewater treatment. Iron is a potential energy source and an essential substrate for anammox bacteria. Microbial iron cycling, which includes iron-oxidizing bacteria (FeOB) and iron-reducing bacteria (FeRB) (Table S1), plays a key role in global nitrogen and iron cycling. Currently, ammonium oxidation coupled with the reduction of ferric iron (Fe (III)) can produce N_2, NO_2^-, or NO_3^- (termed as Feammox) in intertidal wetlands, tropical forest soil, and paddy soils (Ding et al. 2014; Li et al. 2015; Yang et al. 2012). Since the generation of N_2 is more energetically favorable than the production of NO_3^- or NO_2^-, Feammox is considered a potentially significant contributor to nitrogen removal in soils. However, whether Feammox can be used for nitrogen removal for NH_4^+-rich wastewater in wastewater treatment plants remains unverified. This inspired us to explore the role of Feammox in an Anammox- anaerobic sequencing batch reactor (ASBR) system in the presence of different levels of Fe (III) supplementation.

Anammox and Fe (III)-related microbial communities include several rRNA and functional genes, which have played pivotal roles in nitrogen and iron cycling, namely, FeOB 16S rRNA (*Acidimicrobium* spp. and *Ferrovum myxofaciens*), FeRB 16S rRNA (*Albidiferax ferrireducens*, *Geobacter* spp., and *Acidiphilium* spp.), anammox 16S rRNA, archaea ammonia monooxygenase (AOA-*amoA*), ammonia monooxygenase (AOB-*amoA*), nitrite oxidoreductase (*nxrA*), periplasmic nitrate reductase (*napA*), membrane-bound nitrate reductase (*narG*), dissimilatory nitrite reductase (*nrfA*), copper-containing nitrite reductase (*nirK*), nitrite reductase (*nirS*), and nitrous oxide reductase (*nosZ*) (Kandeler et al. 2006; Melton et al. 2014; Zhi et al. 2015). Nevertheless, the long-term effect of Fe (III) on these genes and any ecological association between these functional genes remains unclear.

Molecular biological methods which have been widely used to investigate microbial communities during the anammox process (Kartal et al. 2012) involve fluorescence in situ hybridization (FISH), denaturing gradient gel electrophoresis (DGGE), and sequencing after cloning. With the rapid development of next-generation sequencing, metagenomic studies have been applied to investigate the microbial community structures in full-scale wastewater treatment plants (Ye and Zhang 2013; Zhang et al. 2011). Some species of anammox bacteria have already been assembled using metagenomic shotgun sequencing (Guo et al. 2016; Strous et al. 2006). Nevertheless, little is known about the dynamics of the taxonomical and functional microbial community under different Fe (III) supplementation conditions. Knowledge of microbial community structures and how they are impacted by different Fe (III) supplementation is therefore essential for understanding the feasibility of using Feammox in an Anammox-ASBR system.

Given the above arguments, the present study was conducted with the following objectives: (1) to assess the effects of Fe (III) concentrations on anammox growth rates and activity using batch tests, (2) to evaluate the treatment performance of nitrogen removal under different Fe (III) supplementation in an Anammox-ASBR system, (3) to quantify the variation of rRNA and functional genes in an Anammox-ASBR system and to investigate the ecological associations between nitrogen and iron-related functional genes, and (4) to reveal the dynamics of nitrogen- and iron-related microbial communities in the presence of different Fe (III) supplementation conditions.

Methods

Anammox biomass

The anammox biomass used in this study was obtained from a laboratory-scale SBR that had been in operation for over 2 years. The reactor was incubated in a greenhouse under mesophilic conditions (35 ± 2 °C), with mineral medium and trace element solutions (I and II) (Van de Graaf et al. 1996). The hydraulic retention time (HRT), influent pH, NH_4^+-N, and NO_2^--N concentrations were 4 h, 7.4 ± 0.21, 199 ± 4.5 mg-N/L, and 221 ± 3.6 mg-N/L, respectively. The removal efficiencies of NH_4^+-N and NO_2^--N were 94 ± 0.2 and 96 ± 0.3 %,

respectively. The nitrogen removal loading rate was approximately 2.52 kg-TN (total nitrogen) m^{-3} d^{-1}. Finally, the phyla of "*Canditatus Brocadia sinica*" and "*Kuenenia stuttgartiensis*" comprised the dominant anammox bacteria in this anammox system by 16S rRNA sequencing. These anammox 16S rRNA sequences have been deposited into GenBank (accession number KP721346-KP721365).

Batch tests and kinetic evaluation

The enriched anammox biomass was washed with 0.9 % NaCl solution until the Fe^{3+}, NH_4^+-N, and NO_2^--N concentrations were undetectable. Then, the biomass was centrifuged at 12,000 rpm for 15 min under ambient temperature. The supernatant was discarded, and the biomass pellet was re-suspended in nitrogen-free mineral medium (7.3 ± 0.2). The mineral medium was prepared by purging with N_2 gas (99.99 %) for 20 min and was left in an anaerobic glove box prior to the experiments. In addition, stock solutions of substrates (ammonium and nitrite) were also prepared in the anaerobic chamber prior to the Fe (III) addition. In the short-term experiments, the re-suspended biomass (10 ml) was dispensed into 100-ml serum glass vials sealed with silicon-teflon gaskets and polypropylene caps (Shu et al. 2015). Then, the same amounts of ammonium and nitrite but with different Fe (III) concentrations (details in Table 1) were added into the vials with a syringe. The stock solution of Fe (III)-EDTA was prepared using the mixture of $FeCl_3 \cdot 6H_2O$ and EDTA·2Na. The nitrogen-free mineral medium was added to a final volume of 60 ml. Finally, all the vials were incubated at 32 °C and shaken at a speed of 120 rpm in the dark. Samples were taken from the vials hourly over 9 h to analyze the NH_4^+-N consumption profiles.

To investigate the impacts of Fe (III) addition on anammox bacteria, the specific anammox growth rates under different Fe (III) stresses were measured according to the Haldande substrate inhibition kinetics (Eq. 1) model (Andrews 1968; Tang et al. 2013).

$$\mu_{AN} = \frac{\mu_{AN,\ max}}{1 + \frac{K_{Fe}}{S_{Fe}} + \frac{S_{Fe}}{K_I}} \quad (1)$$

where K_{Fe} is the half-saturation constant, mM; S_{Fe} is the Fe (III) concentration, mM; K_I is the inhibition constant, mM; and μ_{AN} and $\mu_{AN,max}$ are the specific and maximum anammox growth rates, d^{-1}, respectively.

Long-term experiment procedure

For long-term experiments, ~900 ml anammox-ASBR seeding sludge was derived from the above lab-scale anammox SBR of an initial mixed liquid suspended solids (MLSSs) and mixed liquor volatile suspended solids (MLVSSs) of 3.5 and 2.0 g/L, respectively. The new ASBR system has a working volume of 2.6 L and was also operated under mesophilic conditions (35 ± 2 °C) in a greenhouse. The reactor was continuously fed with the trace element solution and mineral medium containing 100 mg-N/L NH_4^+-N and 120 mg-N/L NO_2^--N but with different Fe (III) concentrations (details in Table 1).

The new Anammox-ASBR system was run in a 6-h cycle, including a 10-min feeding period, 340-min anaerobic reaction with a mechanic mixing (120 rpm), 20-min settling, and 10-min discharge of 1.5-L effluent. The stock solution of Fe (III)-EDTA was added into this system automatically at the end of each feeding period to maintain influent Fe (III) concentrations of 0, 0.04, 0.06, 0.08, 0.10, and 0.12 mM (Table 1).

DNA extraction and quantitative real-time PCR

At the end of each phase, three independent sludge samples were collected from the Anammox-ASBR system. Then, three individual genomic DNA samples were extracted from 0.5-g anammox biomass for each sample using the FastDNA® SPIN Kit for Soil (MP Biomedicals, Illkirch, France) according to the manufacturer's instructions. The extracted DNA concentration was measured by a NanoDrop Spectrophotometer ND-1000 (Thermo Fisher Scientific, USA), and the DNA purity was determined through 1.0 % agarose gel electrophoresis. Prior to the quantification of the 16S rRNA and functional genes, equal amounts of three independent genomic DNA samples for each phase were pooled.

Table 1 Batch test and long-term experiment conditions

	NH_4^+-N (mg l^{-1})	NO_2^--N (mg l^{-1})	Fe (III) levels (mM)
Batch experiments			
Batch test 1	80	96	0.04
Batch test 2	80	96	0.06
Batch test 3	80	96	0.08
Batch test 4	80	96	0.10
Batch test 5	80	96	0.12
Batch test 6	80	96	0.14
Long-term experiments			
Phase I (1–20 days)	100	120	0
Phase II (21–40 days)	100	120	0.04
Phase III (41–60 days)	100	120	0.06
Phase IV (61–80 days)	100	120	0.08
Phase V (81–100 days)	100	120	0.10
Phase VI (101–120 days)	100	120	0.12

Compared with RNA-based techniques, DNA-based methods are more robust alternatives for determining microbial activity for the given environmental conditions. Thus, quantitative real-time PCR, a DNA-based technology, was applied to investigate the "key players" in the Anammox-ASBR system under Fe (III) supplementation. The absolute abundance of bacterial 16S rRNA, anammox bacteria 16S rRNA, AOB-*amoA*, AOA-*amoA*, nxrA, *narG*, *napA*, *nrfA*, *nirS*, *nirK*, *nosZ*, FeOB 16S rRNA, and FeRB 16S rRNA were quantified using Mastercycler ep realplex (Eppendorf, Hamburg, Germany) based on the SYBR® Green II method. The plasmids and calibration curves of the rRNAs and functional genes of interest have been described in previous research (Shu et al. 2016). The qPCR amplification was performed in 10 μl reaction mixtures, containing 5 μl SYBR® Premix Ex Taq™ II (Takara, Japan), 0.25 μl of each primer, 1 μl of genomic DNA, and 3.5 μl dd H_2O. The detailed primers and protocols for qPCR are listed in Table S2. To check reproducibility, triplicate PCR reactions were performed for each DNA and double-distilled water was used as the negative control.

PCR amplification and Illumina MiSeq sequencing

The genomic DNA samples collected on days 20, 40, 60, 80, 100, and 120 were conducted with Illumina MiSeq analysis to explore the dynamics of the taxonomical and functional microbial community in an Anammox-ASBR reactor. The hyper-variable V3-V4 region of the bacterial 16S rRNA was amplified using bacterial primers 338F (5′-ACTC CTACGGGAGGCAGCA-3′) and 806R (5′-GGAC TACHVGGGTWTCTAAT-3′). The PCR amplification reaction mixture and protocols followed previous studies (Shu et al. 2016). Each PCR reaction was run in triplicate.

After amplification, PCR products were pooled in equimolar ratios and were purified with an AxyPrep DNA Gel Extraction Kit (Axgen, USA). Then, amplicon libraries were constructed and sequenced using the MiSeq Illumina platform (300-bp paired-end reads) (Shanghai Personal Biotechnology Co., Ltd., Shanghai, China). All raw reads have been deposited into the National Center for Biotechnology Information (NCBI) Sequence Read Archive (SRA) database (http://www.ncbi.nlm.nih.gov/sra/) with an accession number of SRR3565903.

Sequence processing and bioinformatics analysis

Following sequencing, the raw paired-end reads were merged using FLASH (version 1.2.11; http://ccb.jhu.edu/software/FLASH/), and then, quality filtering of reads was conducted using the QIIME pipeline (version 1.9.0; http://qiime.org/scripts/assign_taxonomy.html). After the quality filtration, the remaining high-quality reads were clustered into operational taxonomic units (OTUs) by setting the similarity threshold at 97 % using UCLUST (version 5.2.32; http://drive5.com/usearch/manual/uclust_algo.html). Then, the taxonomic classification was performed using the QIIME pipeline via the Silva SSU database (http://www.arb-silva.de), with a confidence threshold of 70 % (Bai et al. 2014). To avoid unequal sampling depth biases during comparison of microbial diversity and to ensure adequate sample depth (Lee et al. 2012), an appropriate subsample depth (28,306 reads) was selected for further analysis. Subsequently, alpha diversity statistics included Chao 1 estimator, ACE estimator, Shannon index, Simpson index, Good's coverage, and rarefaction curves at a distance of 0.03 were measured for six samples using the Mothur (version 1.30.1; http://www.mothur.org/wiki/Main_Page). Beta diversity statistics such as principal coordinates analysis (PCoA) and (un)weighted UniFrac distance metrics were also calculated using the Mothur platform. Furthermore, the microbial features were mapped using METAGENassist (http://www.metagenassist.ca/METAGENassist/faces/Home.jsp).

Chemical and statistical analyses

The influent and effluent water samples were taken from the Anammox-ASBR system on a daily basis; the samples were first filtered through a 0.45-μm pore diameter membrane and then were analyzed immediately. The concentrations of NH_4^+-N, NO_2^--N, and NO_3^--N were analyzed using Hach TNT 830 reagent, Hach TNT 820 reagent, and Hach TNT 820 reagent, respectively, with a spectrophotometer (DR 2800, Hach, USA). The MLSS and MLVSS of anammox sludge were determined according to the Standard Methods (Rice et al. 2012). The deviations between the measured NH_4^+-N concentrations and the model predictions were evaluated by minimizing the sum of squares using the secant method embedded in AQUASIM 2.1d (Reichert 1998), which was also used to estimate the μ_{AN} value.

Pearson's correlation coefficients were applied to measure the significant correlations between rRNAs and functional genes using SPSS Statistics 20 (http://www-01.ibm.com/software/analytics/spss/; IBM, USA). Redundancy discriminant analysis (RDA), which was applied to evaluate the relationships between operational parameters and microbial communities, was performed using R (version 3.3; https://www.r-project.org/) with the "vegan" and "permute" packages in RStudio (version 0.98; https://www.rstudio.com/).

Results

The effects of Fe (III) addition on anammox activity

For a better understanding of anammox bacterial activity under different Fe (III) supplementation, the short-term batch

experiments were performed in 9 h. Figure 1a–f depicts the measured and kinetic fitted NH_4^+-N consumption profiles from the six batch tests under different Fe (III) concentrations. In general, the NH_4^+-N concentrations decreased linearly in these short-term experiments with different reduction rates. As shown in Fig. 1, the kinetic fittings were correlated with the corresponding experimental measurements.

After 9-h incubation, with the increase of Fe (III) concentrations from 0.04 mM (Fig. 1a) to 0.10 mM (Fig. 1d), the fitted specific anammox growth rates increased from 0.1343 to 0.1709 d^{-1}. However, the specific anammox growth rates declined from 0.1709 to 0.1411 d^{-1} when the Fe (III) concentrations were further increased from 0.10 to 0.14 mM (Fig. 1d–f). Compared with μ_{AN} (0.1343 d^{-1}) in batch test 1, the results indicate that the maximum μ_{AN} ($\mu_{AN,max}$) was 0.1709 d^{-1} in the presence of Fe (III) of 0.10 mM, which was 21.41 % higher than that observed in batch test I (Fig. 1a). Additionally, the μ_{AN} in batch test 5 and batch test 6 were also higher than that in batch test I. Therefore, these results indicate that lower Fe (III) concentrations (0.04–0.10 mM) may significantly improve the anammox activity. And, although anammox activity could be suppressed by high Fe (III) concentration (0.10–0.14 mM) stresses, it is noteworthy that anammox bacteria can tolerate to higher Fe (III) (Fe (III) > 0.10 mM) constraints.

The estimated specific anammox growth rates (μ_{AN}) in six batch experiments with corresponding Fe (III) concentrations are summarized in Fig. 1g. The observed dependence of μ_{AN} on the Fe (III) concentration can be described using Haldande substrate inhibition kinetics with an R^2 value of 0.9623.

$$\mu_{AN} = \frac{0.2999}{1 + \frac{0.0444}{S_{Fe}} + \frac{S_{Fe}}{0.203}} \tag{2}$$

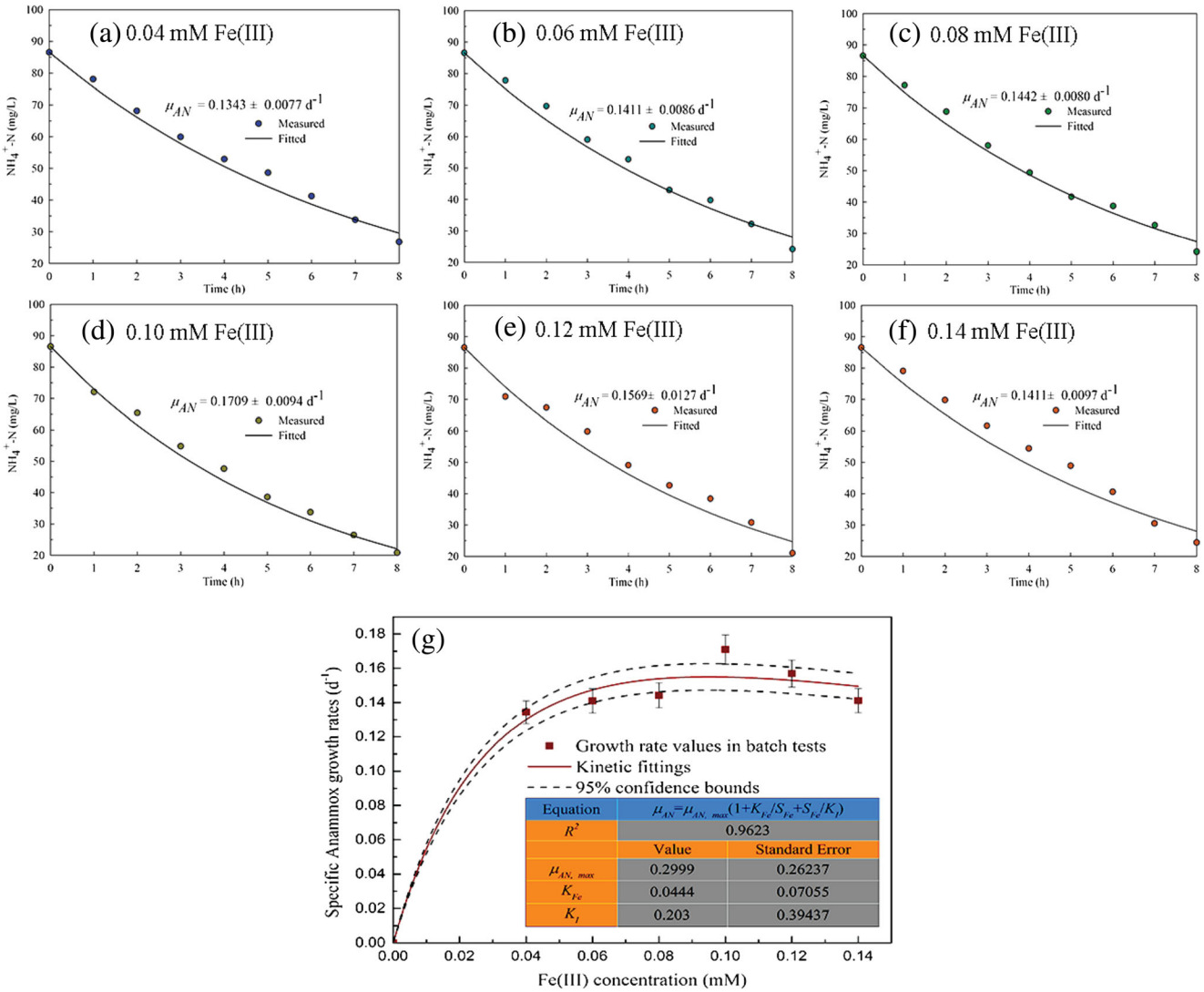

Fig. 1 **a**–**f** The kinetic fitted and measured NH_4^+-N consumption profiles in six 9-h batch tests under different Fe (III) stresses. **g** The actually observed and model-fitted relationships between Fe (III) conditions and specific anammox growth rates using substrate inhibition kinetics

where 0.2999 d^{-1} is the maximum growth rate of anammox under Fe (III) stress, 0.0444 mM is the half-saturation concentration constant, and 0.203 mM is the inhibition constant. Figure 1g also presents the predicted 95 % confidence interval, further indicating that anammox growth rate under Fe (III) stress can be described by Eq. 1. In addition, the results also indicate that 0.10 mM is the optimal concentration of Fe (III) of anammox bacteria growth.

Treatment profiles and reactor performance

In order to explore the treatment performance of Anammox-ASBR for nitrogen removal under Fe (III) supplementation, the reactor was operated during six phases over a time period of 120 days as summarized in Table 1. The nitrogen concentrations, nitrogen removal efficiencies, nitrogen transformation rates, and nitrogen loading rates are shown in Fig. 2. During phase I (1–20 days), the average NH_4^+-N, NO_2^--N, and total nitrogen (TN) removal efficiencies were 86.79 ± 0.76, 88.48 ± 0.21, and 75.99 ± 0.64 %, respectively. Correspondingly, the NH_4^+-N, NO_2^--N, and TN transformation rates were 0.346 ± 0.004, 0.423 ± 0.007, and 0.667 ± 0.011 kg-N/(m^3 d), respectively. The nitrogen removal rate and nitrogen loading rate were 1.119 ± 0.009 and 0.932 ± 0.010 kg-N/(m^3 d). The stoichiometric ratio of NH_4^+-N, NO_2^--N, and NO_3^--N was 1:(1.311 ± 0.024):(0.296 ± 0.009), which was in agreement with the theoretical values for the anammox process (Van de Graaf et al. 1996). However, the stoichiometric ratio in this study is higher than the results from Lotti T et al. and Oshiki M et al. (Lotti et al. 2014a; Oshiki et al. 2016).

During phase II (21–40 days), 0.04 mM of Fe (III) was supplied. As shown in Fig. 2, the NH_4^+-N, NO_2^--N, and TN efficiencies were 87.96 ± 0.36, 91.74 ± 0.25, and 79.08 ± 1.06 %, respectively. In addition, the NH_4^+-N, NO_2^--N, and TN transformation rates increased slightly to 0.347 ± 0.006, 0.428 ± 0.010, and 0.681 ± 0.001 kg-N/(m^3 d), respectively. The stoichiometric ratio of NH_4^+-N, NO_2^--N, and NO_3^--N was 1:(1.234 ± 0.043):(0.271 ± 0.022).

During phase III (41–60 days), the Fe (III) concentration was increased to 0.06 mM. As shown in Fig. 2, the NH_4^+-N,

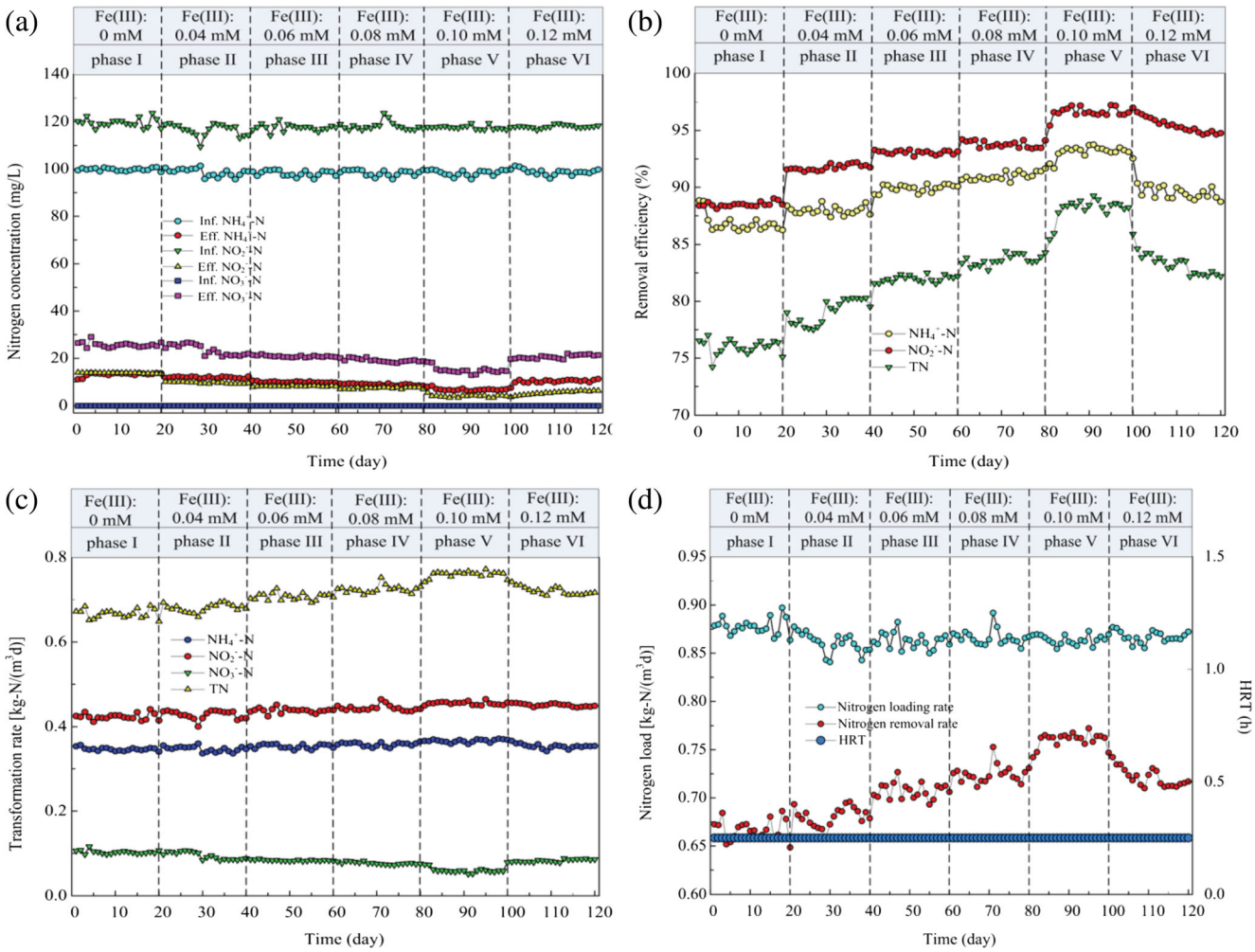

Fig. 2 Long-term treatment performance of Anammox-ASBR system under different Fe (III) stresses. **a** Nitrogen concentrations, **b** nitrogen removal efficiency, **c** nitrogen transformation rates, and **d** nitrogen load

NO_2^--N, and TN efficiencies increased again slightly to 89.92 ± 0.32, 93.07 ± 0.17, and 81.98 ± 0.29 %, respectively. Moreover, the NH_4^+-N, NO_2^--N, and TN transformation rates also increased slightly.

During phase IV (61–80 days), the nitrogen removal efficiency and nitrogen transformation rates were observed to have increased yet further. As shown in Fig. 2, the NH_4^+-N, NO_2^--N, and TN efficiencies increased to 90.98 ± 0.35, 93.78 ± 0.29, and 83.66 ± 0.46 %, respectively. In addition, the NH_4^+-N, NO_2^--N, and TN transformation rates also increased to 0.358 ± 0.005, 0.443 ± 0.007, and 0.725 ± 0.009 kg-N/(m^3 d), respectively.

During phase V (81–100 days), the Fe (III) concentration was set to 0.10 mM in the influent. In comparison with phases I–IV, the NH_4^+-N, NO_2^--N, and TN efficiencies increased to 90.98 ± 0.35, 93.78 ± 0.29, and 83.66 ± 0.46 %, respectively. Accordingly, the stoichiometric ratio of NH_4^+-N, NO_2^--N, and NO_3^--N was 1:(1.241 ± 0.019):(0.166 ± 0.018). The nitrogen load rate and nitrogen removal rate increased to 0.864 ± 0.005 and 0.760 ± 0.007 kg-N/(m^3 d), respectively.

During phase VI (101–120 days), the influent Fe (III) concentration was further increased to 0.12 mM. Compared with phase V, the NH_4^+-N, NO_2^--N, and TN efficiencies declined to 89.51 ± 0.52, 95.39 ± 0.61, and 83.16 ± 0.78 %, respectively. Accordingly, the stoichiometric ratio of NH_4^+-N, NO_2^--N, and NO_3^--N increased to 1:(1.274 ± 0.018):(0.234 ± 0.010). However, the effluent NH_4^+-N concentration and NO_3^--N production increased significantly to 10.35 ± 0.50 and 20.69 ± 0.78 mg/L, respectively.

Quantification of 16S rRNA and functional genes

The absolute abundance of bacterial 16S rRNA, anammox 16S rRNA, AOA *amoA*, AOB *amoA*, *nxrA*, *napA*, *narG*, *nrfA*, *nirK*, *nirS*, *nosZ*, FeOB 16S rRNA (*Acidimicrobium* spp. and *F. myxofaciens*), and FeRB 16S rRNA (*A. ferrireducens*, *Geobacter* spp., and *Acidiphilium* spp.) is shown in Fig. 3. During phases I–VI, the absolute abundance of bacterial 16S rRNA genes was in the range of 3.56×10^9 to 6.06×10^9 copies/(g wet sludge), indicating that the bacterial abundance remained in the same order of magnitude under different Fe (III) stresses. The gene copy numbers of anammox bacteria varied significantly during the six phases, ranging between 3.36×10^8 and 2.12×10^9 copies/(g wet sludge). These results indicate that the absolute abundance of anammox bacteria in phase V was nearly one to two orders of magnitude higher than that in phases I–IV and phase VI (Fig. 3a).

The copy numbers of three nitrification groups, including AOA *amoA*, AOB *amoA*, and *nxrA* genes, are summarized in Fig. 3b. With the increase of Fe (III) concentrations from 0 to 0.12 mM during phases I–VI, the absolute abundance of AOA *amoA* and AOB *amoA* genes varied significantly, ranging from 4.46×10^1–3.74×10^2 to 1.71×10^4–2.55×10^7 copies/(g wet sludge), respectively (Fig. 3b). However, the copy number of the *nxrA* gene was in the same order of magnitude throughout phases I–VI.

As shown in Fig. 3c, the dissimilatory nitrogen reduction genes include *nrfA*, *napA*, and *narG* genes. With the increase of Fe (III) from 0 to 0.10 mM during phases I–V, the copy number of *nrfA* genes increased from 7.98×10^6–3.57×10^7 copies/(g wet sludge). However, the copy number of *nrfA* genes declined to 3.57×10^7 copies/(g wet sludge) in phase VI. In addition, the copy numbers of *napA* and *narG* genes were in the range of 3.83×10^5–8.82×10^5 and 2.83×10^5–1.17×10^6 copies/(g wet sludge), respectively. Notably, the copy numbers of the *napA* and *narG* genes were higher in phase V than that in phases I–IV and phase VI, indicating that dissimilatory nitrogen reduction processes have contributed to nitrogen removal under the Fe (III) supplementation (0–0.10 mM) in the Anammox-ASBR system.

Three denitrification groups, including *nirK*, *nirS*, and *nosZ* genes, are displayed in Fig. 3d. With the increase of Fe (III) from 0 to 0.10 mM, the copy number of *nirK*, *nirS*, and *nosZ* genes increased from 2.00×10^6 to 6.62×10^6, 1.05×10^8 to 2.35×10^8, and 2.41×10^4 to 4.49×10^4 copies/(g wet sludge), respectively. However, the absolute abundance of the *nirK*, *nirS*, and *nosZ* genes slightly declined in phase VI as the Fe (III) concentration further increased to 0.12 mM. These results showed that the absolute abundance of denitrification genes slightly increased, suggesting that the activity of denitrifies could be promoted with the addition of 0.04–0.10 mM of Fe (III).

As illustrated in Fig. 3e, the FeOB group included *Acidimicrobium* spp. and *F. myxofaciens*. During phases I–VI, the copy numbers of *Acidimicrobium* spp. and *F. myxofaciens* ranged from 3.85×10^8–9.17×10^8 and 1.54×10^6–4.38×10^6 copies/(g wet sludge), respectively. The results showed that *Acidimicrobium* spp. had maximum copy numbers in phase IV, but *F. myxofaciens* was more abundant in phase V.

As shown in Fig. 3f, the copy number of FeRB groups involved *A. ferrireducens*, *Geobacter* spp., and *Acidiphilium* spp. Results showed that the copy number of *A. ferrireducens*, *Geobacter* spp., and *Acidiphilium* spp. ranged from 3.07×10^8 to 5.80×10^8, 4.86×10^5 to 3.85×10^6, and 1.04×10^4 to 4.38×10^4 copies/(g wet sludge), respectively. Additionally, the absolute abundance of the *A. ferrireducens* increased gradually during phases I–V, while it declined in phase VI. The copy numbers of *Geobacter* spp. increased in phases I–VI as the Fe (III) increased from 0 to 0.12 mM. Furthermore, the absolute abundance of *Acidiphilium* spp. was higher in phase III than in the other five phases. These results indicate that the activity of FeRB could be enhanced with the addition of appropriate Fe (III) supplementation.

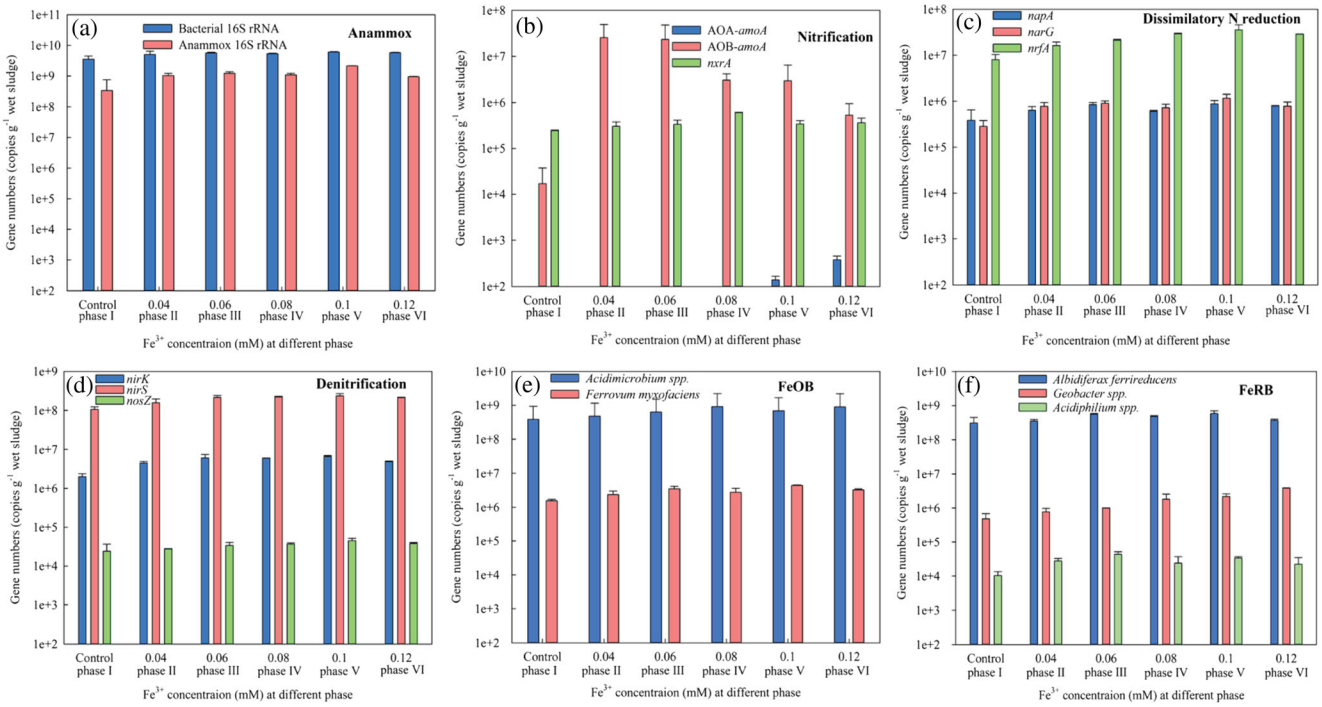

Fig. 3 Quantitative analysis of functional genes under different Fe (III) stresses. The *error bars* represent the standard deviation calculated from three independent experiments. **a** Absolute abundance of bacterial 16S rRNA and anammox 16S rRNA. **b** Absolute abundance of nitrification functional genes, including AOA amoA, AOB amoA, and *nxrA* genes. **c** Absolute abundance of dissimilatory nitrate reduction functional genes, including *napA*, *narG*, and *nrfA* genes. **d** Absolute abundance of denitrification functional genes, including *nirK*, *nirS*, and *nosZ* genes. **e** Absolute abundance of FeOB 16S rRNA (*Acidimicrobium* spp. and *Ferrovum myxofaciens*). **f** Absolute abundance of FeRB 16S rRNA (*Albidiferax ferrireducens*, *Geobacter* spp., and *Acidiphilium* spp.)

Relationship between Fe (III) and microbial communities succession

In this study, MiSeq sequencing was applied to investigate the relationship between Fe (III) and microbial community succession. As shown in Table 2, after quality filtering and chimera trimming, 28,306–33,426 high-quality reads were obtained from six samples. Values of the OTUs, Good's coverage, Shannon, Chao 1, ACE, and Simpson at a cutoff level of 3 % were also calculated and summarized in Table 2. The OTUs were in the range of 750–930 for six samples in phases I–IV. Good's coverage of the six samples ranged from 97 to 99 %, indicating that the diversity of the microbial community was covered by the current sequence libraries. Additionally, the Shannon, Chao 1, ACE, and Simpson indices were in the range of 4.69–5.32, 1195.92–1449.02, 1328.27–1559.07, and 0.87–0.92, respectively, demonstrating that the richness values varied by 0.8–1.0 times among these samples. Based on the OTUs, rarefaction curves were calculated for these six samples and were presented in Fig. S1. The results showed that the rarefaction curves did not reach a plateau after subsampling, indicating that new bacterial phylotypes could continue to emerge after the sequencing depth exceeded 28,306 reads.

Based on the unweighted UniFrac distance metrics, PCoA were performed to explore the similarities of samples under different Fe (III) stresses. The results of PCoA analysis with

Table 2 Raw and effective reads, plus number of OTUs, Good's coverage, Shannon, Chao1, ACE, and Simpson of six sludge samples

Sample ID	Raw reads	Effective reads	Subsampling	OTUs	Good's coverage	Shannon	Chao 1	ACE	Simpson
Phase _I	42,931	32,274	28,306	787	0.98	4.69	1,407.88	1,442.05	0.87
Phase _II	39,983	30,366	28,306	810	0.97	5.21	1,449.02	1,559.07	0.91
Phase _III	37,509	28,306	28,306	750	0.99	4.71	1,290.44	1,399.13	0.88
Phase _IV	44,503	33,426	28,306	760	0.98	4.91	1,195.92	1,328.27	0.90
Phase _V	38,505	28,422	28,306	806	0.99	4.98	1,359.53	1,438.93	0.90
Phase _VI	43,761	31,315	28,306	930	0.99	5.32	1,430.23	1,529.89	0.92

maximum variation of 15.88 % (PC1) and 19.92 % (PC2) are shown in Fig. 4a. The results indicate that phase I, phases II–IV, and phase V–VI tended to cluster together, respectively.

As shown in Fig. 4b, least discriminant analysis (LDA) was applied to investigate the significant taxonomic differences under Fe (III) stresses conditions. Based on the results of major taxa (abundance >1 %), the phyla *Chlorobi*, *Chloroflexi*, *Planctomycetes*, and *Proteobacteria* were dominant in phases I–VI. *Ignavibacteria*, *Anaerolineae*, *Phycisphaerae*, and *Alphaproteobacteria* were the major classes in phases I–VI. *Ignavihacteriaies*, *Phycisphaeraies*, *Brocadiales*, *Rhodobacterales*, and *Burkholderiales* were more abundant at the order level in phases I–VI. The families *Ignavibacteriaceae*, *Brocadiaceae*, *Hyphomonadaceae*, and *Comamonadaceae* were dominant in phases I–VI. *Candidatus* Brocadia and *Candidatus* Kuenenia were dominant anammox phylotypes in phases I–VI.

Dynamics of taxonomical and functional microbial communities

All effective sequences from different phases were further assigned to the corresponding taxa levels (from phylum to genus). As shown in Fig. 5, *Chloroflexi* was the most abundant phylum in the six phases, accounting for 34.39–39.31 % (averaging 36.54 %) of the total sequences. The other dominant phyla included *Planctomycetes* (30.73–35.31 %, averaging 32.26 %), *Proteobacteri*a (15.40–18.61 %, averaging 16.95 %), and *Chlorobi* (4.78–6.58 %, averaging 5.57 %). These results are consistent with previous studies (Bai et al. 2014; Zhang et al. 2011), showing that *Chloroflexi*, *Planctomycetes*, *Proteobacteri*a, and *Chlorobi* were the dominant (89.53–92.67 %) phyla in wastewater treatment systems. Other major phyla (average abundance >1 %) found in phases I–VI included *Acidobacteria* (1.98 %) and *Bacteroidetes* (2.30 %). Several other phyla, namely, *Actinobacteria*, *Armatimonadetes*, *Firmicutes*, *Gemmatimonadetes*, *Nitrospirae*, *OD1*, *OP11*, *TM7*, *Verrucomicrobia*, and *WS6*, were the major phyla (abundance >1 %) in one of the six samples. The abundance of other phyla was lower than 1 % in phases I–VI.

As Fe (III) concentrations increased from 0.04 to 0.10 mM, the percentage of *Planctomycetes* increased from 30.73 to 35.31 %. Then, it declined to 31.90 % as the Fe (III) concentration increased to 0.12 mM, while the percentage of *Planctomycetes* in phase VI was still higher than that in phase I. These results indicate that *Planctomycetes* has a tolerance for higher Fe (III) (>0.10 mM) stresses and that the appropriate addition of Fe (III) (0.04–0.10 mM) was more favorable to anammox bacteria species in the phylum of *Planctomycetes*.

As shown in Fig. S2a, a total of 97 microbial classes were obtained in phases I–VI, with 29 of them being dominant. These classes accounted for 95.84–97.16 % of classified sequences. Within *Proteobacteria*, *α-Proteobacteria* (4.41–5.73 %), *β-Proteobacteria* (6.88–8.14 %), *γ-Proteobacteria* (0.99–1.31 %), and *δ-Proteobacteria* (2.71–4.57 %) are common to all six phases. Of the filtered sequences, a total of 167 bacterial orders and 234 bacterial families were identified, with 29 of them being of dominant, as Figs. S2b and 2c. The results showed that *Solibacteraceae*, *Cytophagaceae*, *Ignavibacteriaceae*, *Brocadiaceae*, *Comamonadaceae*, *Rhodocyclaceae*, and *Haliangiaceae* were more abundant and shared by all six samples in all phases.

Among the 291 assigned genera, 87 were most abundant. Interestingly, only 45 genera were commonly shared by

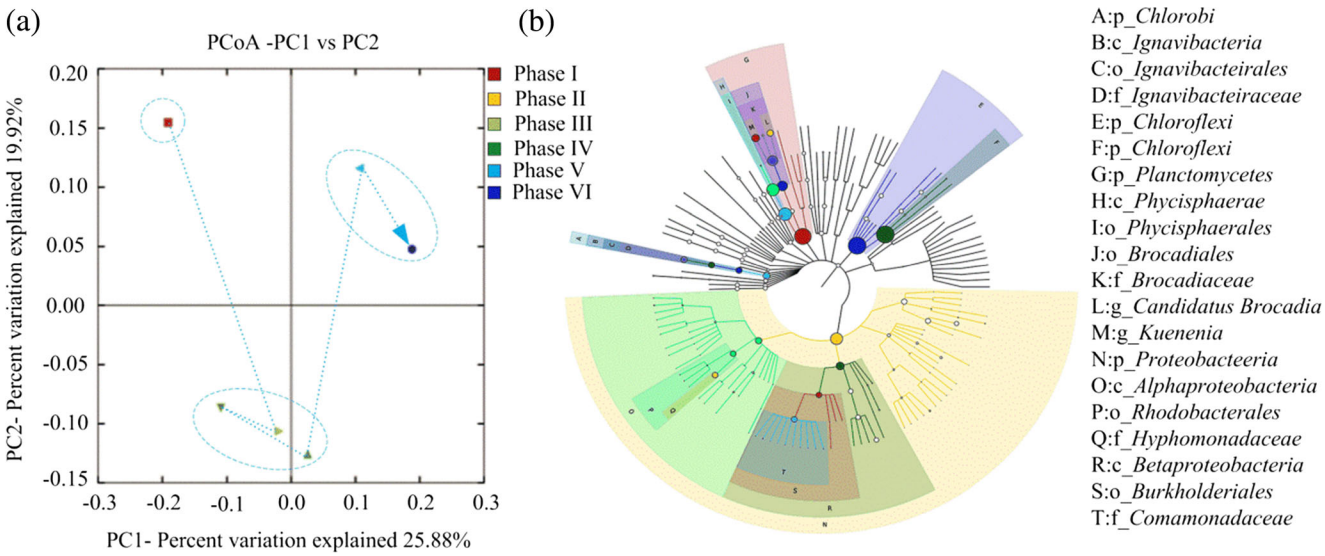

Fig. 4 Distinct microbial patterns of the different Fe (III) stress conditions. **a** Unweighted UniFrac distance principal coordinate analysis (PCoA) of microbial communities in the six phases. **b** Least discriminant analysis (LDA) effect size taxonomic cladogram comparing all consortia categorized according to different Fe(III) supplementation

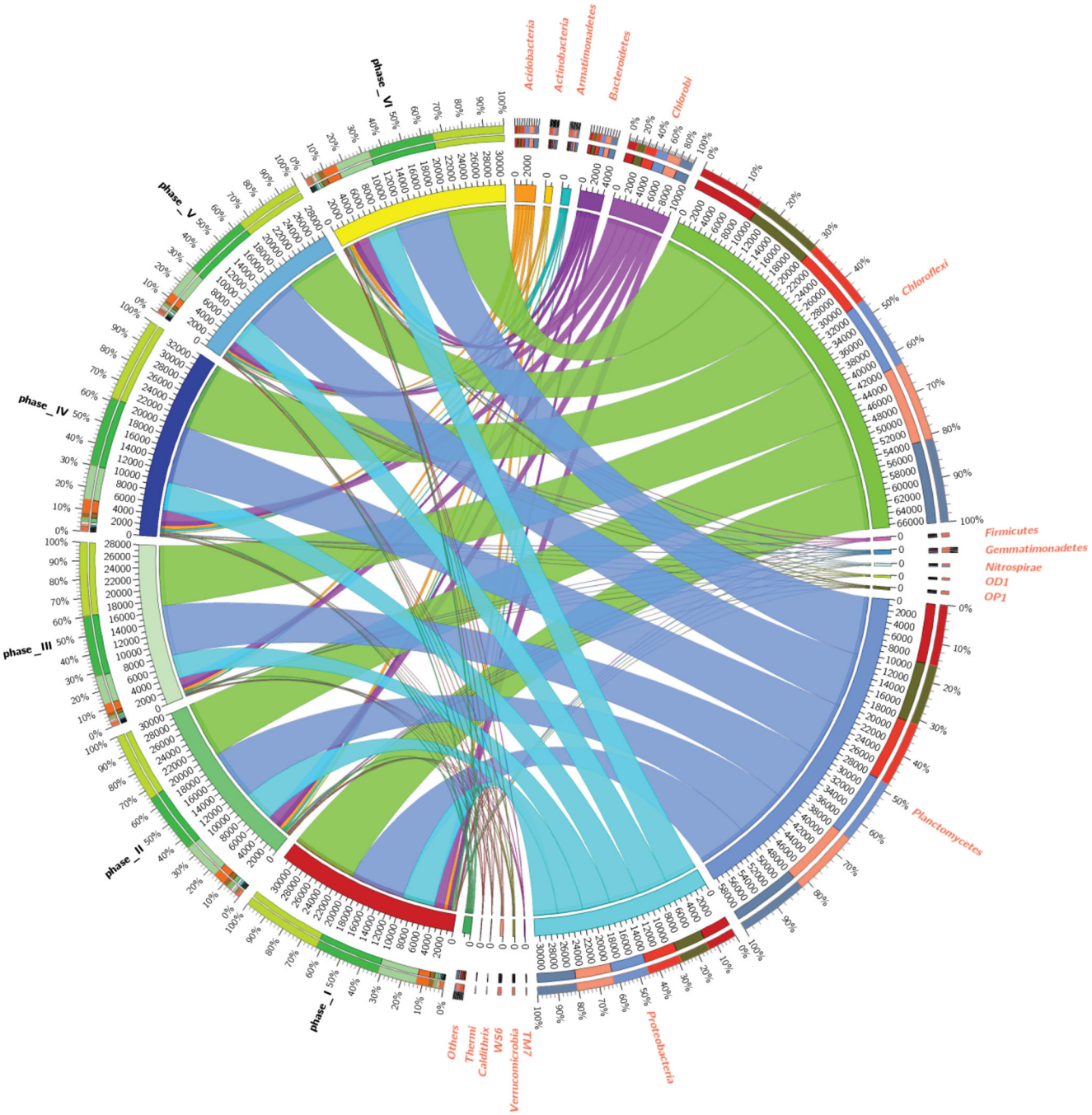

Fig. 5 Distribution of phyla in the six phases based on the taxonomy annotation via SILVA SSU database using RDP classifier. The thickness of each ribbon represents the abundance of each taxon. The absolute tick above the inner segment and relative tick above the outer segment stand for the read abundances and relative abundance of each taxon, respectively. Others refer to those unclassified reads. The data were visualized using Circos (version 0.67; http://circos.ca/)

more than 2 samples. Here, the 45 most dominant genera in the six samples were selected and their functions were analyzed. As shown in Fig. 6, 51.7 % of generalists were identified as belonging to 11 functional groups, including 4 anammox, 1 AOB, 7 denitrifier, 1 DNRA, 2 FeOB, 2 FeRB, 4 fermenters, 1 nitrogen-fixing bacteria, 1 NOB, 1 organic-degrading bacteria, 1 PAH-degrading bacteria, and 19 unassigned functional groups.

Based on these results, METAGENassist was applied to further explore the metabolic functions of the identified generalists. In addition, results from the PCoA showed that the phase I, phases II–IV, and phase V–VI tended to cluster together, respectively. These generalists in METAGENassist were therefore assigned as group A, group B, and group C. As shown in Fig. 7a–c, the metabolic activities in group A, group B, and group C included ammonia oxidizers, aromatic hydrocarbon

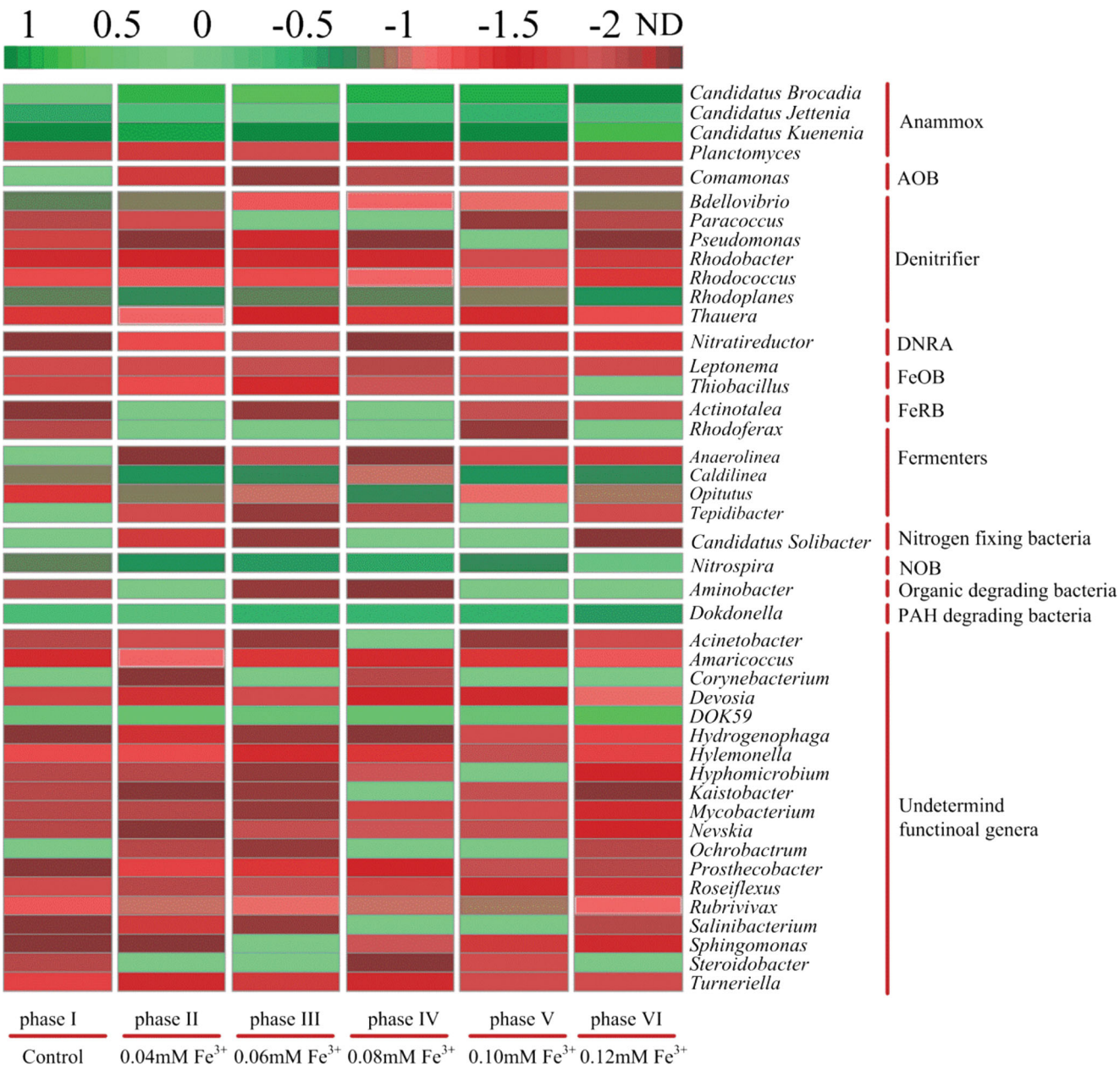

Fig. 6 The relative abundance (log scale) of functional genera in the six phase samples

degraders, dehalogenaters, nitrite reducers, nitrogen fixers, streptomycin producer, sulfate reducers, sulfide oxidizer, sulfur oxidizers, sulfur reducers, and xylan degraders. But certain of these, notably ammonia oxidizers (44.6 %), aromatic hydrocarbons degraders (2.0 %), nitrite reducers (41.0 %), sulfate reducers (24.2 %), sulfide oxidizers (38.2 %), sulfur reducers (1.4 %), and denitrifyers (0.06 %) were higher in groups B and C.

Discussion

The anammox process has been successfully applied in full-scale wastewater treatment plants to reduce carbon and energy input for nitrogen removal (Kartal et al. 2013; Lotti et al. 2014b). Several strategies have been applied to enhance the specific anammox growth rates. Much research has focused on how to encourage fast start-up anammox processes with these suggested strategies. It was found that the addition of Fe (III) to batch assays drastically improved the specific anammox activity, with a maximum increase of 533.2 % for an Fe (III) dose of 3.68 mg l^{-1} (Chen et al. 2014). In addition, the excess Fe (III) drastically diminished the deammonification performance (Liu and Horn 2012). However, the relationship between Fe (III) and specific anammox growth rates has not been fully explored before. Thus, the metabolic activity of anammox and the dynamics of functional microbial

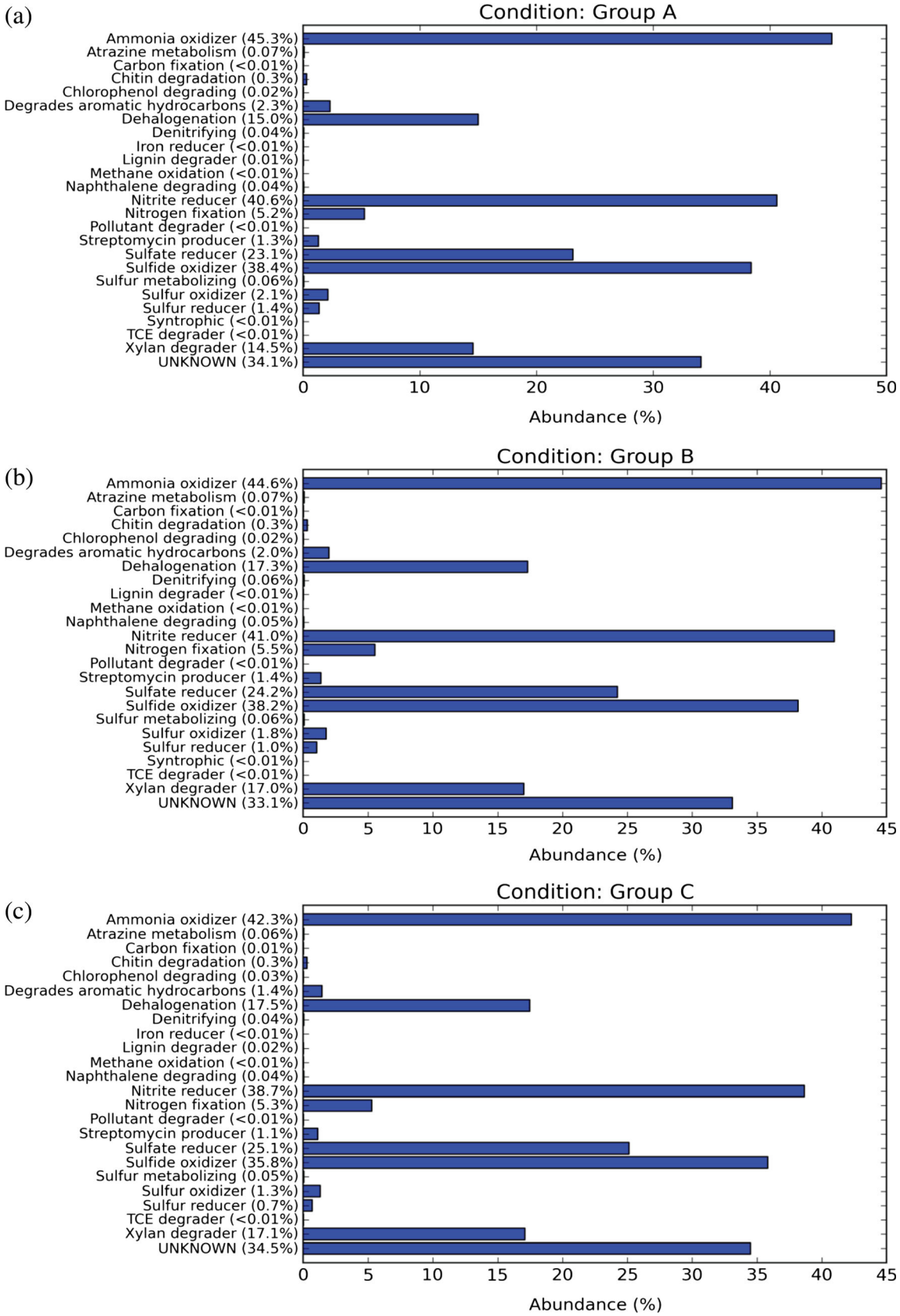

Fig. 7 Comparison of the metabolic groups in the bacterial communities among six phases in the phase I (group A), phases II–IV (group C), and phases V–VI (group C), according to the METAGENassist analysis

communities under different Fe (III) supplementation were investigated in this study.

We first conducted a kinetic analysis of the specific anammox growth rates using batch tests at different Fe (III) supplementation levels. Since the concentrations of NH_4^+-N, NO_2^--N, and amounts of anammox biomass would have impacts on the anammox growth rates, these operational parameters were controlled to be at same levels in the batch tests. As a result, the influence of Fe (III) on anammox activity was investigated under other factor-limited conditions, revealing a substrate inhibition correlation between the specific anammox rates and Fe (III) supplementation (R^2 = 0.9623). Previous studies have reported that iron is an essential element for anammox bacteria. Moreover, Fe (III) insoluble FeOOH can act as an electron acceptor for the acetyl-CoA pathway for anammox bacteria, particularly for *Candidatus K. stuttgartiensis* (Kartal et al. 2013). Here, there are two possible pathways explaining the Fe (III) uptake for anammox bacteria in Anammox-ASBR system. Firstly, Andrews et al. found that siderophores have low molecular mass and have affinity towards Fe (III), and the pathway of siderophore-mediated iron uptake is commonly found in gram-negative bacteria. Hence, Fe (III)-siderophore complexes can be bound by specific outer membrane (OM) receptors and then delivered to the cytosol acetyl-CoA pathway by ATP-binding cassettes. Secondly, gram-negative anammox bacteria possess a type of iron transport system (Feo), which is very different from the Fe (III)-siderophore-mediated systems. In this transport system, Fe (III) is reduced to Fe (II) via extracellular reductases and then taken up by Feo-mediated systems (Andrews et al. 2003). Furthermore, Fe (III) reduction plays a pivotal role in electron transport for the generation of cytochrome C, which has been considered as an essential part of some key functional enzymes for the growth of anammox bacteria like *Candidatus K. stuttgartiensis* (Kuenen 2008). Therefore, combined analysis from the short- and long-term experiments suggested that Fe (III) addition (<0.10 mM) could be an effective approach to promote the growth rates of anammox bacteria in an Anammox-ASBR system, as shown in Figs. 1 and 2.

The results of qPCR further support the above analyses. The absolute abundance of anammox bacteria in phase I was nearly one order of magnitude lower than that observed in phase V. Previous studies have reported that anaerobic ammonium oxidation coupled with nitrite reduction (termed as Feammox) is an important microbial pathway of nitrogen removal in intertidal wetlands, tropical forest soil, and paddy soils (Ding et al. 2014; Li et al. 2015; Yang et al. 2012). However, little is known about the role of Feammox in Anammox-ASBR system under Fe (III) supplementation. Thus, it is hypothesized that Feammox has the potential to removal nitrogen in the Anammox-ASBR system with Fe (III) addition. Iron-reducing bacteria which are dissimilatory Fe (III) reducers include *A. ferrireducens*, *Geobacter* spp., and *Acidiphilium* spp. (Melton et al. 2014). The results from the qPCR and Pearson's correlation coefficients support this hypothesis, as shown in Fig. 3 and Table 3. The gene copy number of *A. ferrireducens* in phase V was nearly two times more than that observed in phase I. The absolute abundance of *Geobacter* spp. in phase VI was nearly one order of magnitude higher than that observed in phase I. With the increase of Fe (III) concentration from 0 to 0.12 mM, the gene copy numbers of *Acidiphilium* spp. increased in phases I–V but slightly decreased in phase V–VI. Therefore, the appropriate Fe (III) addition not only enhanced the anammox growth rates but also promoted the activity of FeRB (iron-reducing bacteria). Furthermore, as presented in Table 3, the pairs of anammox-(*narG* + *napA*), anammox-*nrfA*, anammox-*nosZ*, anammox-FeRB, (*narG* + *napA*)-(*nirK* + *nirS*), (*narG* + *napA*)-*nosZ*, *nrfA*-(*nirK* + *nirS*), *nrfA*-*nosZ*, (*nirK* + *nirS*)-*nosZ*, and (*nirK* + *nirS*)-FeRB showed significant positive correlation. Their Pearson's correlation coefficients (*r*) exceeded 0.820 ($p < 0.05$).

The conversion of NO_3^--N to NO_2^--N is catalyzed by the *narG* and *napA* genes. The NO_3^--N was consumed in this conversion, and the substrate NO_2^--N was provided for anammox bacteria, nitrite reducers, and other microorganism. Thus, the results indicated that the anammox-(*narG* + *napA*) pair showed a significant protocooperation. In the step of dissimilatory nitrite reduction, the conversion of NO_2^--N to NH_4^+-N is catalyzed by the *nrfA* gene (Smith et al. 2007). It consumed NO_2^--N and provided NH_4^+-N for another nitrogen removal pathway. The anammox-*nrfA* pair is therefore has a mutually beneficial relationship (Table 3). These results were consistent with the findings of Zhi et al., in which the coupling of DNRA and anammox is a noteworthy pathway contributing to nitrogen loss in tidal flow-constructed wetlands (Zhi et al. 2015).

In the first step of denitrification, *nirK* and *nirS* genes are the key genes responsible for conversion of NO_2^--N to NO (Kandeler et al. 2006). The *nosZ* gene, encoding the N_2O reductase, is the key gene in the conversion of N_2O to NO or N_2, which is often used as a gene marker for the final denitrification step. Functional genes like anammox, *narG*, *napA*, *nirK*, and *nirS* can provide the indirect or direct substrates NO_3^--N, NO_2^--N, and NO for the *nosZ* gene. In addition, the *narG* and *napA* genes consumed NO_3^--N and provided the substrate NO_2^--N for *nirK* and *nirS* genes. DNRA and denitrifying bacteria are chemolithotrophic, and both of them have the capacity to remove organic carbon in the given conditions. Therefore, the pairs of anammox-*nosZ*, (*narG* + *napA*)-(*nirK* + *nirS*), (*narG* + *napA*)-*nosZ*, *nrfA*-(*nirK* + *nirS*), *nrfA*-*nosZ*, and (*nirK* + *nirS*)-*nosZ* showed a collaboration relationship.

Marc Strous et al. found that some anammox bacteria such as *K. stuttgartiensis* have the capacity to reduce Fe (III) to Fe (II) with formate as the electron donor (Strous et al. 2006). In addition, Fe (III) can be reduced to Fe (II) with NH_4^+-N as the electron donor and it can then provide NO_3^--N and NO_2^--N

Table 3 Pearson's correlation coefficients between 16S rRNAs and functional genes

	Anammox	*AOA + AOB*	*nxrA*	*narG + napA*	*nrfA*	*nirK + nirS*	*nosZ*	*FeOB*	*FeRB*
Anammox	1.0000								
AOA + AOB	0.0733	1.0000							
nxrA	0.1909	−0.2177	1.0000						
narG + napA	0.910*	0.2502	0.1550	1.0000					
nrfA	0.820*	−0.2749	0.5555	0.8058	1.0000				
nirK + nirS	0.7971	−0.0118	0.5734	0.874*	0.933**	1.0000			
nosZ	0.851*	−0.3149	0.4220	0.826*	0.980**	0.912*	1.0000		
FeOB	0.3482	−0.3678	0.7822	0.4599	0.8090	0.7934	0.7312	1.0000	
FeRB	0.843*	0.1314	0.3441	0.7979	0.7025	0.828*	0.7502	0.3854	1.0000

Pearson's correlation coefficient values with $p < 0.01$ and $p < 0.05$ are shown in blue ($n = 6$)

*Correlation is significant at the 0.05 level (two-tailed)

**Correlation is significant at the 0.01 level (two-tailed)

for denitrification and anammox bacteria (Yang et al. 2012). Additionally, as shown in Fig. 3b, results from RDA indicated that anammox bacteria have positive correlations with *A. ferrireducens*, *Geobacter* spp., and *Acidiphilium* spp. It is notable that these three FeRB also showed positive relationships with the NH_4^+-N, NO_2^--N, and TN removal rates. Taken together, combined analysis from Pearson's coefficients and RDA analysis indicated that coupling of anammox, dissimilatory nitrogen reduction, and FeRB are the potential pathways for TN loss in this Anammox-ASBR system. However, the quantitative molecular mechanism of Feammox- and Fe (III)-reducing rates in Anammox-ASBR system needs further study using ^{15}N-labeled ammonium-based isotopic-tracing and acetylene inhibition techniques.

To explore the dynamics of microbial community structures under different Fe (III) supplementation conditions, especially for anammox bacteria, 338F-806R primer was used for Illumina MiSeq sequencing. The *Chloroflexi* (34.39–39.31 %) was the most abundant phylum in the Anammox-ASBR system, followed by *Planctomycetes* (30.73–35.31 %), *Proteobacteria* (15.40–18.61 %), and *Chlorobi* (4.78–6.58 %). In a study of an Anammox-UASB system, Cao et al. found that *Chloroflexi* (25.77–29.14 %), *Bacteroidetes* (9.92–28.01 %), *Proteobacteria* (22.1–23.58 %), and *Planctomycetes* (1.09–8.39 %) (Cao et al. 2016) were the dominant phyla. It had been reported that the phylum *Chloroflexi* was capable of degrading complex organic matter. A previous study revealed that uncultured *Chloroflexi* has the capacity to degrade and utilize cellular compounds derived from dead anammox cells (Kindaichi et al. 2012) using a ^{14}C-tracing technique. It was found that the phylum *Chloroflexi* can serve as an anaerobic core and that it plays a key role during anaerobic sludge granulation (Gao et al. 2011). In addition, the findings of Chu et al. showed that the members of *Chloroflexi* constitute a large portion (>25 %) of the bacterial community in a one-stage nitritation-anammox system, indicating that the role of *Chloroflexi* could not be neglected in an autotrophic nitrogen removal system (Chu et al. 2015). In this study, the abundance of *Chloroflexi* in phase III was higher than that observed in the other five phases, indicating that lower Fe (III) concentration (<0.08 mM) was beneficial to *Chloroflexi*.

The *Proteobacteria* was a highly abundant phylum in the present study. Four classes of *Proteobacteria*, including *α-Proteobacteria*, *β-Proteobacteria*, *γ-Proteobacteria*, and *δ-Proteobacteria*, varied significantly in phases I–VI. However, *β-Proteobacteria* was the most dominant *Proteobacteria*. These findings were consistent with previous studies (Ye and Zhang 2013; Zhang et al. 2011), revealing that *β-Proteobacteria* was the most dominant class in municipal wastewater treatment systems using 454 pyrosequencing. In terms of *β-Proteobacteria* in the anammox sludge, Isantal et al. revealed that *β-Proteobacteria* accounted for approximately 14 % of the bacteria in an Anammox-SBR system based on 454 pyrosequencing (Isanta et al. 2015). In contrast, the results from the Biswas et al. showed that *γ-Proteobacteria* was the most abundant group (52 %) in a moving bed biofilm reactor (MBBR) system for nitrogen removal (Biswas et al. 2014). The discrepancy between the present study and the previous studies mentioned above may be due to different operational parameters, such as the type of bioreactor, characteristics of influent wastewater, volatile fatty acid concentrations, and heavy metal concentrations.

Chlorobi and *Bacteroidetes* are also relatively abundant phyla in the Anammox-ASBR system. Previous studies showed that *Chlorobi* and *Bacteroidetes* are omnipresent in anammox systems (Isanta et al. 2015). It was found that *Chlorobi* and *Bacteroidetes* were considered to be responsible for the granulation of anammox flocculent biomass. Furthermore, based on the results of a metagenomic assembly approach, Speth et al. revealed that *Chlorobi* and *Bacteroidetes* might enhance anammox performance and reduce nitrate and nitrous oxide reduction in an anammox system (Speth et al. 2016).

Planctomycetes are found throughout the ecosystem, including in marine, freshwater systems, and soil habitats, and it even exists in some extreme environments (Fuerst and Sagulenko 2011). Current studies suggest that anammox *Planctomycetes* are major contributors to the global nitrogen cycle and are of great significance to the autotrophic nitrogen removal process in wastewater treatment plants (Kuenen 2008). Thus, it was predicted that *Planctomycetes* would be predominant in the Anammox-ASBR reactor which operated over 120 days. As expected, *Planctomycetes* (30.73–35.31 %) was another major phylum in Anammox-ASBR system, which agreed with the findings of Isanta et al. (Isanta et al. 2015). As depicted in Fig. S3a, results showed that the phylum of *Planctomycetes* has positive correlations with NH_4^+-N, NO_3^--N, and TN removal rates, indicating that *Planctomycetes* makes a contribution to nitrogen removal in the Anammox-ASBR system.

Candidatus Brocadia, *Candidatus* Kuenenia, *Candidatus* Scalindua, *Candidatus* Anammoxoglobus, and *Candidatus* Jettenia are currently considered as five representative genera of anammox bacteria (Kartal et al. 2013). The results from Fig. 6 showed that *Candidatus* Brocadia and *Candidatus* Kuenenia were the dominant genera and accounted for 1.99–7.80 and 4.1–8.3 % of genus in Anammox-ASBR system, respectively. The relative abundance of *Candidatus* Brocadia varied slightly in phases I–VI with the highest relative abundance of 7.79 % of total genera in phase VI. This was due to the *S*-strategy survival ability of *Candidatus* Brocadia, which prefers this strategy to the Fe (III) supplementation. With the increase of Fe (III) from 0.04 to 0.10 mM, *Candidatus* Kuenenia's relative abundance increased from 6.8 to 7.7 %. However, the relative percentage of *Candidatus* Kuenenia declined to 4.15 % in phase VI. Obviously, *Candidatus* Kuenenia prefers the *K*-strategy to the appropriate Fe (III) addition (<0.10 mM). In addition, the percentage of *Candidatus* Jettenia increased from 0.24 to 0.56 % with the increase of Fe (III) concentration from 0 to 0.06 mM. Zhao et al. analyzed the interaction of the iron reduction and nitrogen removal pathway of *Candidatus* Kuenenia and determined that *Candidatus* Kuenenia was capable of iron respiration (Zhao et al. 2014). Stours et al. confirmed the versatility of *Candidatus* Kuenenia by uncoverting its ability to use formate as an electron donor for iron respiration (Strous et al. 2006). It was found that Fe (III) addition might result in the community succession of anammox species. Taken together, it was evident that lower Fe (III) supplementation (<0.10 mM) is beneficial for *Candidatus* Kuenenia and *Candidatus* Jettenia, and *Candidatus* Brocadia can tolerate higher Fe (III) supplementation (>0.10 mM). Nevertheless, the molecular mechanism of iron respiration in the Anammox-ASBR system needs to be further investigated.

To our knowledge, this study is the first to systematically investigate the dynamics of microbial communities in an Anammox-ASBR system under different Fe (III) supplementation conditions via MiSeq sequencing of the 16S rRNA gene. In the present study, results from short- and long-term experiments indicated that Fe (III) addition (<0.10 mM) could be an effective approach to enhance the growth of anammox bacteria. Meanwhile, it was observed that the Haldande substrate inhibition kinetics can be used to describe relationship between Fe (III) concentration and specific anammox bacteria growth. Combined analyses from the qPCR and Pearson's correlation coefficients revealed that coupling anammox, dissimilatory nitrogen reduction to ammonium, and iron reduction were the potential explanatory factors for nitrogen loss in the Anammox-ASBR system. Moreover, MiSeq sequencing revealed that *Chloroflexi*, *Planctomycetes*, *Proteobacteria*, and *Chlorobi* were the dominant phyla in this system. It should be noted that *Candidatus* Brocadia and *Candidatus* Kuenenia adopt different growth strategies under different Fe (III) supplementation. Overall, these results suggest that a Fe (III)-based strategy could potentially be used to enhance the nitrogen removal performance for the application of anammox-related technologies. The molecular mechanism for potential iron respiration in *Candidatus* Kuenenia and *Candidatus* Jettenia should be further investigated by employing metagenomic and metatranscriptomic approaches.

Acknowledgments This research was financially supported by the National Key Technology R&D program (2012BAC09B05) and the Science and Technology Project of Qinghai Province (2009 N207). The authors are grateful to Hong Yue for her assistance in equipment supply and MiSeq analysis.

Compliance with ethical standards This article does not contain any studies with human participants or animals performed by any of the authors.

Conflict of interest The authors declare that they have no conflict of interest.

References

Ali M, Oshiki M, Rathnayake L, Ishii S, Satoh H, Okabe S (2015) Rapid and successful start-up of anammox process by immobilizing the minimal quantity of biomass in PVA-SA gel beads. Water Res 79:147–157

Andrews JF (1968) A mathematical model for the continuous culture of microorganisms utilizing inhibitory substrates. Biotechnol Bioeng 10(6):707–723

Andrews SC, Robinson AK, Rodríguez-Quiñones F (2003) Bacterial iron homeostasis. FEMS Microbiol Rev 27(2–3):215–237

Bai Y, Qi W, Liang J, Qu J (2014) Using high-throughput sequencing to assess the impacts of treated and untreated wastewater discharge on prokaryotic communities in an urban river. Appl Microbiol Biotechnol 98(4):1841–1851

Biswas K, Taylor MW, Turner SJ (2014) Successional development of biofilms in moving bed biofilm reactor (MBBR) systems treating municipal wastewater. Appl Microbiol Biotechnol 98(3):1429–1440

Cao S, Du R, Li B, Ren N, Peng Y (2016) High-throughput profiling of microbial community structures in an ANAMMOX-UASB reactor treating high-strength wastewater. Appl Microbiol Biotechnol:1–11

Chen H, J-J Y, Jia X-Y, Jin R-C (2014) Enhancement of anammox performance by Cu (II), Ni (II) and Fe (III) supplementation. Chemosphere 117:610–616

Chu Z-r, Wang K, Li X-k, Zhu M-t, Yang L, Zhang J (2015) Microbial characterization of aggregates within a one-stage nitritation–anammox system using high-throughput amplicon sequencing. Chem Eng J 262:41–48

Ding L-J, An X-L, Li S, Zhang G-L, Zhu Y-G (2014) Nitrogen loss through anaerobic ammonium oxidation coupled to iron reduction from paddy soils in a chronosequence. Environ Sci Technol 48(18):10641–10647

Duan X, Zhou J, Qiao S, Wei H (2011) Application of low intensity ultrasound to enhance the activity of anammox microbial consortium for nitrogen removal. Bioresour Technol 102(5):4290–4293

Fuerst JA, Sagulenko E (2011) Beyond the bacterium: planctomycetes challenge our concepts of microbial structure and function. Nature reviews. Microbiology 9(6):403–413

Gao D, Liu L, Liang H, W-M W (2011) Aerobic granular sludge: characterization, mechanism of granulation and application to wastewater treatment. Crit Rev Biotechnol 31(2):137–152

Gao F, Zhang H, Yang F, Li H, Zhang R (2014) The effects of zero-valent iron (ZVI) and ferroferric oxide (Fe_3O_4) on anammox activity and granulation in anaerobic continuously stirred tank reactors (CSTR. Process Biochem 49(11):1970–1978

Guo J, Peng Y, Fan L, Zhang L, Ni BJ, Kartal B, Feng X, Jetten MS, Yuan Z (2016) Metagenomic analysis of anammox communities in three different microbial aggregates. Environ Microbiol doi. doi:10.1111/1462-2920.13132

Isanta E, Bezerra T, Fernández I, Suárez-Ojeda ME, Pérez J, Carrera J (2015) Microbial community shifts on an anammox reactor after a temperature shock using 454-pyrosequencing analysis. Bioresour Technol 181:207–213

Jin R-C, Yang G-F, J-J Y, Zheng P (2012) The inhibition of the anammox process: a review. Chem Eng J 197:67–79

Kandeler E, Deiglmayr K, Tscherko D, Bru D, Philippot L (2006) Abundance of *narG*, *nirS*, *nirK*, and *nosZ* genes of denitrifying bacteria during primary successions of a glacier foreland. Appl Environ Microbiol 72(9):5957–5962

Kartal B, van Niftrik L, Keltjens JT, Op den Camp HJ, Jetten MS (2012) Anammox-growth physiology, cell biology, and metabolism. Adv Microb Physiol 60:212

Kartal B, de Almeida NM, Maalcke WJ, den Camp HJO, Jetten MS, Keltjens JT (2013) How to make a living from anaerobic ammonium oxidation. FEMS Microbiol Rev 37(3):428–461

Kindaichi T, Yuri S, Ozaki N, Ohashi A (2012) Ecophysiological role and function of uncultured Chioroflexi in an anammox reactor. Water Sci Technol 66(12):2556–2561

Kuenen JG (2008) Anammox bacteria: from discovery to application. Nature reviews. Microbiology 6(4):320–326

Lee CK, Herbold CW, Polson SW, Wommack KE, Williamson SJ, McDonald IR, Cary SC (2012) Groundtruthing next-gen sequencing for microbial ecology—biases and errors in community structure estimates from PCR amplicon pyrosequencing. PLoS One 7:e44244

Li X, Hou L, Liu M, Zheng Y, Yin G, Lin X, Cheng L, Li Y, Hu X (2015) Evidence of nitrogen loss from anaerobic ammonium oxidation coupled with ferric iron reduction in an intertidal wetland. Environ Sci Technol 49(19):11560–11568

Liu S, Horn H (2012) Effects of Fe (II) and Fe (III) on the single-stage deammonification process treating high-strength reject water from sludge dewatering. Bioresour Technol 114:12–19

Liu Y, Ni B-J (2015) Appropriate Fe (II) addition significantly enhances anaerobic ammonium oxidation (anammox) activity through improving the bacterial growth rate. Sci Rep 5:8204

Lotti T, Kleerebezem R, Lubello C, van Loosdrecht MCM (2014a) Physiological and kinetic characterization of a suspended cell anammox culture. Water Res 60:1–14

Lotti T, Kleerebezem R, van Erp Taalman Kip C, Hendrickx TL, Kruit J, Hoekstra M, van Loosdrecht MC (2014b) Anammox growth on pretreated municipal wastewater. Environ Sci Technol 48(14):7874–7880

Lotti T, Kleerebezem R, Abelleira-Pereira J, Abbas B, van Loosdrecht M (2015) Faster through training: the anammox case. Water Res 81:261–268

Melton ED, Swanner ED, Behrens S, Schmidt C, Kappler A (2014) The interplay of microbially mediated and abiotic reactions in the biogeochemical Fe cycle. Nature reviews. Microbiology 12:797–807

Oshiki M, Satoh H, Okabe S (2016) Ecology and physiology of anaerobic ammonium oxidizing bacteria. Environ Microbiol doi. doi:10.1111/1462-2920.13134

Qiao S, Bi Z, Zhou J, Cheng Y, Zhang J (2013) Long term effects of divalent ferrous ion on the activity of anammox biomass. Bioresour Technol 142:490–497

Reichert P (1998) Aquasim 2.0—user manual, computer program for the identification and simulation of aquatic systems. Swiss Federal Institute for Environmental Science and Technology (EAWAG), Dübendorf, p. 219

Rice EW, Bridgewater L, Association APH (2012) Standard methods for the examination of water and wastewater. American Public Health Association, Washington, DC

Schmidt J, Batstone D, Angelidaki I (2004) Improved nitrogen removal in upflow anaerobic sludge blanket (UASB) reactors by incorporation of anammox bacteria into the granular sludge. Water Sci Technol 49(11–12):69–76

Shu D, He Y, Yue H, Zhu L, Wang Q (2015) Metagenomic insights into the effects of volatile fatty acids on microbial community structures and functional genes in organotrophic anammox process. Bioresour Technol 196:621–633

Shu D, He Y, Yue H, Wang Q (2016) Metagenomic and quantitative insights into microbial communities and functional genes of nitrogen and iron cycling in twelve wastewater treatment systems. Chem Eng J 290:21–30

Smith CJ, Nedwell DB, Dong LF, Osborn AM (2007) Diversity and abundance of nitrate reductase genes (*narG* and *napA*), nitrite reductase genes (*nirS* and *nrfA*), and their transcripts in estuarine sediments. Appl Environ Microbiol 73(11):3612–3622

Speth DR, Guerrero-Cruz S, Dutilh BE, Jetten MS (2016) Genome-based microbial ecology of anammox granules in a full-scale wastewater treatment system. Nat Commun 7:11172

Strous M, Kuenen JG, Jetten MS (1999) Key physiology of anaerobic ammonium oxidation. Appl Environ Microbiol 65(7):3248–3250

Strous M, Pelletier E, Mangenot S, Rattei T, Lehner A, Taylor MW, Horn M, Daims H, Bartol-Mavel D, Wincker P (2006) Deciphering the evolution and metabolism of an anammox bacterium from a community genome. Nature 440(7085):790–794

Tang C-J, Zheng P, Chai L-Y, Min X-B (2013) Thermodynamic and kinetic investigation of anaerobic bioprocesses on anammox under high organic conditions. Chem Eng J 230:149–157

Van de Graaf AA, de Bruijn P, Robertson LA, Jetten MS, Kuenen JG (1996) Autotrophic growth of anaerobic ammonium-oxidizing micro-organisms in a fluidized bed reactor. Microbiology 142(8):2187–2196

van de Graaf AA, de Bruijn P, Robertson LA, Jetten MS, Kuenen JG (1997) Metabolic pathway of anaerobic ammonium oxidation on the basis of 15 N studies in a fluidized bed reactor. Microbiology 143(7):2415–2421

Van der Star WR, Abma WR, Blommers D, Mulder J-W, Tokutomi T, Strous M, Picioreanu C, Van Loosdrecht M (2007) Startup of reactors for anoxic ammonium oxidation: experiences from the first full-scale anammox reactor in Rotterdam. Water Res 41(18):4149–4163

Yang WH, Weber KA, Silver WL (2012) Nitrogen loss from soil through anaerobic ammonium oxidation coupled to iron reduction. Nat Geosci 5(8):538–541

Ye L, Zhang T (2013) Bacterial communities in different sections of a municipal wastewater treatment plant revealed by 16S rDNA 454 pyrosequencing. Appl Microbiol Biotechnol 97(6):2681–2690

Zhang T, Shao M-F, Ye L (2011) 454 pyrosequencing reveals bacterial diversity of activated sludge from 14 sewage treatment plants. The ISME journal 6(6):1137–1147

Zhao R, Zhang H, Li Y, Jiang T, Yang F (2014) Research of iron reduction and the iron reductase localization of anammox bacteria. Curr Microbiol 69:880–887

Zhi W, Yuan L, Ji G, He C (2015) Enhanced long-term nitrogen removal and its quantitative molecular mechanism in tidal flow constructed wetlands. Environ Sci Technol 49(7):4575–4583